Multiple Feature-Enhanced SAR Imaging Using Sparsity in Combined Dictionaries

Sadegh Samadi, *Member, IEEE*, Müjdat Çetin, *Member, IEEE*, and Mohammad Ali Masnadi-Shirazi, *Member, IEEE*

***Abstract*—Nonquadratic regularization-based image formation is a recently proposed framework for feature-enhanced radar imaging. Specific image formation techniques in this framework have so far focused on enhancing one type of feature, such as strong point scatterers, or smooth regions. However, many scenes contain a number of such feature types. We develop an image formation technique that simultaneously enhances multiple types of features by posing the problem as one of sparse representation based on combined dictionaries. This method is developed based on the sparse representation of the *magnitude* of the scattered complex-valued field, composed of appropriate dictionaries associated with different types of features. The multiple feature-enhanced reconstructed image is then obtained through a joint optimization problem over the combined representation of the magnitude and the phase of the underlying field reflectivities.**

***Index Terms*—Complex-valued imaging, image reconstruction, sparse signal representation, synthetic aperture radar (SAR).**

I. Introduction

THE anticipated high data rates and the time-critical nature of emerging synthetic aperture radar (SAR) tasks motivate the use of automated processing techniques in extracting information from a SAR image for an accurate and efficient interpretation of the scene. There is growing interest in such techniques, wherein features extracted from the formed imagery are used for tasks such as automatic target detection and recognition. The conventional image formation algorithms in traditional SAR systems are based on the Fourier transform [1], which leads to images limited in resolution by the system bandwidth, and exhibiting noise and sidelobe artifacts. This kind of processing does not take into account either any available contextual information, or the final objectives of the SAR mission regarding the automated decisions or interpretations to be made.

Recently, significant effort has been spent toward new approaches for SAR image formation. An important motivation for these approaches has been improving the resolution beyond the Fourier limit, which has resulted in the development of a number of superresolution methods. Examples of such methods include subspace projection techniques [2], parameter estimation or spectral estimation techniques [3], and data extrapolation techniques [4]. The essence of these methods is the consideration of some parametric models for SAR images or underlying targets and posing the SAR image formation as a parameter estimation problem. Most of these methods consider a model that assumes that the underlying field can be considered as a combination of point scatterers. Therefore, most of these image formation approaches enhance pointlike features of the underlying fields; however, they reduce gain on nonpointlike features, and they usually fail to enhance shape-based (SB) features of images containing distributed targets [5].

Nonquadratic regularization-based image formation is a recently proposed framework for feature-enhanced radar imaging [5]. This framework offers a number of advantages over conventional imaging, including superresolution, robustness to uncertain or limited data, and enhanced image quality. Specific image formation techniques in this framework have so far focused on enhancing one type of feature in the imaged scene, such as strong point scatterers, or regions with smoothly varying reflectivity values. However, many scenes contain, and hence require joint enhancement of, a number of such feature types.

In this letter, we develop an image formation technique that simultaneously enhances multiple types of features in the scene. By viewing the image formation problem as a sparse signal representation problem, similar in spirit to [6] but in combined dictionaries, this is achieved by using appropriate dictionaries that combine multiple types of features. In particular, we consider dictionary combinations that jointly represent spatially focused and spatially distributed scene features. The mathematical formulation of this problem is developed in this letter, and multiple feature-enhanced reconstructed images are obtained through a joint optimization over the combined representation of the magnitude and the phase of the complex-valued image. Section II provides the details of our mathematical framework and our solution to the optimization problems encountered in this framework. Section III presents our experimental results, and conclusions are presented in Section IV.

II. Framework of Multiple Feature-Enhanced SAR Imaging

This section describes our mathematical formulation for multiple feature-enhanced SAR imaging. New techniques such as nonquadratic regularization [5] have mostly focused on enhancement of one type of feature in the process of image formation.

Manuscript received September 8, 2011; revised December 26, 2011; accepted March 1, 2012. Date of publication December 25, 2012; date of current version February 20, 2013. This work was supported in part by the Scientific and Technological Research Council of Turkey under Grant 105E090 and in part by the Turkish Academy of Sciences Distinguished Young Scientist Award.

S. Samadi is with the Department of Electrical and Electronics Engineering, Shiraz University of Technology, Shiraz 71557-13876, Iran (e-mail: samadi@sutech.ac.ir).

M. Çetin is with the Faculty of Engineering and Natural Sciences, Sabanci University, 34956 Istanbul, Turkey (e-mail: mcetin@sabanciuniv.edu).

M. A. Masnadi-Shirazi is with the School of Electrical and Computer Engineering, Shiraz University, Shiraz 71348-51154, Iran (e-mail: masnadi@shirazu.ac.ir).

Digital Object Identifier 10.1109/LGRS.2012.2225016

Recently, a technique for SAR imaging based on sparse signal representation has been developed [6]. This work, which introduces the sparse representation (SR) approach for the complex-valued inverse problem of SAR image formation, has shown the capability of the SR approach for producing high-quality SAR images and exhibiting robustness to uncertain or limited data. Extending this work, here, a framework for multiple feature-enhanced SAR imaging is developed based on the SR of the magnitude of the scattered field in terms of appropriate dictionaries associated with different types of features.

We should point out that the work in [5] is based on two fixed regularization terms (one for point enhancement and one for region enhancement), implying a particular choice for the dictionaries. All the freedom one has in that approach is to select the weights of the two regularization terms. On the other hand, in the new approach of this letter, we can: 1) employ a variety of different dictionaries; and (2) use them in such a way that only atoms from one dictionary could be active in a particular spatial region.

A. SAR Observation Model

Two common observation models for SAR imaging problem that have been used in the literature are the geometric theory of diffraction (GTD)-based model and the ill-posed linear model. The former, which is motivated by both physical optics and the GTD, regards the target scattering centers and amplitudes as parameters of a point scattering model [7]. The latter, which is motivated by tomographic formulation of SAR, regards the complex-valued undegraded image of the underlying scene as unknown. The GTD-based model has been mostly used in superresolution methods, which have successfully improved pointlike features of the underlying field. However, this model is not very appropriate for methods that are intended to enhance (e.g., SB) features of distributed targets.

In recent works [5], [6], the ill-posed linear model has been successfully used in methods that improve nonpointlike features of distributed targets; hence, here, we use this model, which provides an appropriate basis for our purpose of enhancing multiple types of features in the reconstructed image. In particular, the linear noisy observation model used in this letter is given by

$$\mathbf{y} = \mathbf{H}\mathbf{f} + \mathbf{n} \tag{1}$$

where $\mathbf{y}$ is the sampled range profile, $\mathbf{f}$ is the undegraded radar image of the underlying scene, and $\mathbf{n}$ is the observation noise; all are column stacked as vectors and of complex-valued nature. $\mathbf{H}$ represents the ill-posed discrete SAR projection operator [5].

B. Sparsity in Combined Dictionaries

Consider M features to be simultaneously enhanced in the process of SAR image formation. Although the unknown scene $\mathbf{f}$ in our observation model is complex valued, in most applications, we are interested in features of its magnitude [6]. Therefore, our approach is based on the SR of the magnitude in a combination of appropriate dictionaries

$$|\mathbf{f}| = \sum_{i=1}^{M} \mathbf{\Phi}_i \boldsymbol{\alpha}_i \tag{2}$$

where $\mathbf{\Phi}_i$'s are appropriate dictionaries for our application that can sparsely represent the scene in terms of the features of interest, and $\boldsymbol{\alpha}_i$'s are vectors of representation coefficients. We can write

$$\mathbf{f} = \operatorname{diag}\{\boldsymbol{\beta}\}|\mathbf{f}| = \operatorname{diag}\{|\mathbf{f}|\}\,\boldsymbol{\beta} \tag{3}$$

where $\boldsymbol{\beta}$ is a vector with elements $(\boldsymbol{\beta})_i = \beta_i = e^{j\phi_i}$, and ϕ_i is the unknown phase of $(\mathbf{f})_i$. Substituting (2) and (3) into (1), we obtain

$$\mathbf{y} = \sum_{i=1}^{M} \mathbf{H}\operatorname{diag}\{\boldsymbol{\beta}\}\mathbf{\Phi}_i\boldsymbol{\alpha}_i + \mathbf{n} = \mathbf{H}\operatorname{diag}\{|\mathbf{f}|\}\,\boldsymbol{\beta} + \mathbf{n}. \tag{4}$$

Considering $\boldsymbol{\beta}$ to be known for now, an estimate of $\boldsymbol{\alpha}_i$'s can be found through the following extended basis pursuitlike method [8]:

$$\{\hat{\boldsymbol{\alpha}}_1, \ldots, \hat{\boldsymbol{\alpha}}_M\} = \arg \min_{\boldsymbol{\alpha}_1,\ldots,\boldsymbol{\alpha}_M} \left\| \mathbf{y} - \sum_{i=1}^{M} \mathbf{H}\operatorname{diag}\{\boldsymbol{\beta}\}\mathbf{\Phi}_i\boldsymbol{\alpha}_i \right\|_2^2 + \sum_{i=1}^{M} \lambda_i \|\boldsymbol{\alpha}_i\|_{p_i}^{p_i} \tag{5}$$

where $\|\cdot\|_p$ denotes the ℓ_p-norm, and λ_i's are positive real parameters. We have let $p_i \leq 1$, for $i = 1, \ldots, M$, to be different so that we can choose proper values according to the ability of each dictionary $\mathbf{\Phi}_i$ to sparsely represent the corresponding feature of interest.

Now, considering $|\mathbf{f}|$ (or equivalently $\boldsymbol{\alpha}_i$'s) to be known, an estimate of $\boldsymbol{\beta}$ can be obtained through the following estimator [6]:

$$\hat{\boldsymbol{\beta}} = \arg\min_{\boldsymbol{\beta}} \|\mathbf{y} - \mathbf{H}\operatorname{diag}\{|\mathbf{f}|\}\,\boldsymbol{\beta}\|_2^2 + \lambda' \sum_{i=1}^{N^2} \left(|(\boldsymbol{\beta})_i| - 1\right)^2 \tag{6}$$

where N^2 is the number of elements of vector $\boldsymbol{\beta}$ for an image of size $N \times N$, and λ' is a positive real constant. For the actual problem where both $\boldsymbol{\alpha}_i$'s and $\boldsymbol{\beta}$ are unknown, we define the following multivariate cost function:

$$J_t(\boldsymbol{\alpha}_1, \ldots, \boldsymbol{\alpha}_M, \boldsymbol{\beta}) = \left\| \mathbf{y} - \sum_{i=1}^{M} \mathbf{H}\operatorname{diag}\{\boldsymbol{\beta}\}\mathbf{\Phi}_i\boldsymbol{\alpha}_i \right\|_2^2 + \sum_{i=1}^{M} \lambda_i \|\boldsymbol{\alpha}_i\|_{p_i}^{p_i} + \lambda' \sum_{i=1}^{N^2} \left(|(\boldsymbol{\beta})_i| - 1\right)^2. \tag{7}$$

The estimates of $\boldsymbol{\alpha}_i$'s and $\boldsymbol{\beta}$, hence that of the complex-valued image, can be obtained through the following block coordinate descent approach:

$$\left\{\hat{\boldsymbol{\alpha}}_1^{(l+1)}, \ldots, \hat{\boldsymbol{\alpha}}_M^{(l+1)}\right\} = \arg \min_{\boldsymbol{\alpha}_1,\ldots,\boldsymbol{\alpha}_M} J_t\left(\boldsymbol{\alpha}_1, \ldots, \boldsymbol{\alpha}_M, \hat{\boldsymbol{\beta}}^{(l)}\right) \tag{8}$$

$$\hat{\boldsymbol{\beta}}^{(l+1)} = \arg \min_{\boldsymbol{\beta}} J_t\left(\hat{\boldsymbol{\alpha}}_1^{(l+1)}, \ldots, \hat{\boldsymbol{\alpha}}_M^{(l+1)}, \boldsymbol{\beta}\right) \tag{9}$$

where l denotes the iteration index.

C. Iterative Solution of the Block Coordinate Descent Algorithm

The partial gradient of the multivariate cost function $J_t(\boldsymbol{\alpha}_1,\ldots,\boldsymbol{\alpha}_M,\boldsymbol{\beta})$ with respect to $\boldsymbol{\alpha}_i$ is

$$\nabla_{\boldsymbol{\alpha}_i} J_t(\boldsymbol{\alpha}_1,\ldots,\boldsymbol{\alpha}_M,\boldsymbol{\beta}) = \mathbf{G}_i(\boldsymbol{\alpha}_i)\boldsymbol{\alpha}_i - 2\left(\mathbf{H}\,\mathrm{diag}\{\boldsymbol{\beta}\}\boldsymbol{\Phi}_i\right)^H \left(\mathbf{y} - \sum_{\substack{j=1\\ j\neq i}}^{M} \mathbf{H}\,\mathrm{diag}\{\boldsymbol{\beta}\}\boldsymbol{\Phi}_j\boldsymbol{\alpha}_j\right) \quad (10)$$

where

$$\mathbf{G}_i(\boldsymbol{\alpha}_i) = 2\left(\mathbf{H}\,\mathrm{diag}\{\boldsymbol{\beta}\}\boldsymbol{\Phi}_i\right)^H \times \left(\mathbf{H}\,\mathrm{diag}\{\boldsymbol{\beta}\}\boldsymbol{\Phi}_i\right) + \lambda_i p_i \boldsymbol{\Lambda}(\boldsymbol{\alpha}_i) \quad (11)$$

$$\boldsymbol{\Lambda}(\boldsymbol{\alpha}_i) = \mathrm{diag}\left\{\frac{1}{\left(|(\boldsymbol{\alpha}_i)_k|^2+\varepsilon\right)^{1-p_i/2}}\right\} \quad (12)$$

in which ε is a small positive constant used to avoid the nondifferentiability problem of the ℓ_p-norm around the origin, and $(\boldsymbol{\alpha}_i)_k$'s are the elements of vector $\boldsymbol{\alpha}_i$. Rewriting the gradient terms in (10) for $i=1,\ldots,M$ in matrix form, we reach to the result

$$\nabla_{\widetilde{\boldsymbol{\alpha}}} J_t(\widetilde{\boldsymbol{\alpha}},\boldsymbol{\beta}) = \widetilde{\mathbf{G}}(\widetilde{\boldsymbol{\alpha}})\widetilde{\boldsymbol{\alpha}} - \widetilde{\boldsymbol{y}} \quad (13)$$

in which $\widetilde{\boldsymbol{\alpha}} = [\boldsymbol{\alpha}_1^T \cdots \boldsymbol{\alpha}_M^T]^T$, $\widetilde{\mathbf{G}}(\widetilde{\boldsymbol{\alpha}})$ is a matrix with diagonal submatrix elements $[\widetilde{\mathbf{G}}(\widetilde{\boldsymbol{\alpha}})]_{ii} = \boldsymbol{G}_i(\boldsymbol{\alpha}_i)$ and nondiagonal submatrix elements $[\widetilde{\mathbf{G}}(\widetilde{\boldsymbol{\alpha}})]_{ij} = 2(\mathbf{H}\mathrm{diag}\{\boldsymbol{\beta}\}\boldsymbol{\Phi}_i)^H(\mathbf{H}\mathrm{diag}\{\boldsymbol{\beta}\}\boldsymbol{\Phi}_j)$, and $\widetilde{\mathbf{y}} = [(2(\mathbf{H}\mathrm{diag}\{\boldsymbol{\beta}\}\boldsymbol{\Phi}_1)^H\mathbf{y})^T \cdots (2(\mathbf{H}\mathrm{diag}\{\boldsymbol{\beta}\}\boldsymbol{\Phi}_M)^H\mathbf{y})^T]^T$. Note that $\widetilde{\mathbf{G}}$ in (13) is a function of $\widetilde{\boldsymbol{\alpha}}$ and we cannot find a closed-form solution for $\widetilde{\boldsymbol{\alpha}}$. Using $\widetilde{\mathbf{G}}(\widetilde{\boldsymbol{\alpha}})$ as an approximation to the Hessian, the following quasi-Newton algorithm can be used to solve the optimization problem in (8) iteratively at each step l (we ignore reference to l here for the sake of notational simplicity):

$$\hat{\widetilde{\boldsymbol{\alpha}}}^{(n+1)} = \hat{\widetilde{\boldsymbol{\alpha}}}^{(n)} - \left[\widetilde{\mathbf{G}}\left(\hat{\widetilde{\boldsymbol{\alpha}}}^{(n)}\right)\right]^{-1} \nabla_{\widetilde{\alpha}} J\left(\hat{\widetilde{\boldsymbol{\alpha}}}^{(n)}\right). \quad (14)$$

Substituting (13) into (14), the following iterative algorithm is obtained:

$$\widetilde{\mathbf{G}}\left(\hat{\widetilde{\boldsymbol{\alpha}}}^{(n)}\right)\hat{\widetilde{\boldsymbol{\alpha}}}^{(n+1)} = \widetilde{\mathbf{y}}. \quad (15)$$

Note that l denotes the iteration index of the overall block coordinate descent algorithm for minimizing the cost function in (7), and n denotes the iteration index of the algorithm for solving the subproblem in (8) for each l. Taking the partial gradient of $J_t(\boldsymbol{\alpha}_1,\ldots,\boldsymbol{\alpha}_M,\boldsymbol{\beta})$ with respect to $\boldsymbol{\beta}$ and continuing in a similar way to the above procedure, we can find the following iterative algorithm for solving the optimization problem in (9):

$$\mathbf{G}'\left(\hat{\boldsymbol{\beta}}^{(n)}\right)\hat{\boldsymbol{\beta}}^{(n+1)} = 2\left(\mathbf{H}\mathrm{diag}\{|\mathbf{f}|\}\right)^H\mathbf{y} \quad (16)$$

where

$$\mathbf{G}'(\boldsymbol{\beta}) = 2\left(\mathbf{H}\mathrm{diag}\{|\mathbf{f}|\}\right)^H\left(\mathbf{H}\mathrm{diag}\{|\mathbf{f}|\}\right) + 2\lambda'\left(\mathbf{I} - \mathrm{diag}\left\{\frac{1}{|(\boldsymbol{\beta})_i|}\right\}\right). \quad (17)$$

D. Considerations on Combined Dictionary Selection

The above framework allows the use of combinations of various dictionaries based on the features to be simultaneously enhanced. Two features of particular interest in SAR images are strong point scatterers of man-made targets and smooth regions of different natural regions in the terrain or distributed targets. To select a dictionary, we should consider both its ability to sparsely represent the feature of interest and the likelihood of efficient implementation of the above algorithm using it. We introduce the following two combined dictionaries with these characteristics for joint enhancement of pointlike targets and smooth areas in SAR images.

PR Dictionary: The SB dictionary introduced in [6] could be a good candidate for this purpose; however, it is not computationally efficient. Here, we propose a simpler dictionary, which is much more efficient. This dictionary is a combination of two subdictionaries, namely, a point-based subdictionary and a region-based subdictionary. The point-based subdictionary is a dictionary of isolated point scatterers at all possible positions. Considering our formulation in the previous sections, for a SAR image of size $N\times N$, the size of this subdictionary is $N^2\times N^2$. More specifically, it is an identity matrix of this size. For the region-based subdictionary, we propose using a dictionary or a combination of various dictionaries of local spatial smoothing filters for enhancing smooth regions. Each column of such a dictionary contains elements of an $N\times N$ matrix, with all elements zero except for a local region around a specific pixel, reshaped as a vector. Therefore, each atom in this dictionary takes the shape of the impulse response of a low-pass spatial filter, centered around a particular pixel. Different types of smoothing filters can be used based on the features of the smooth region of interest. Averaging, circular averaging, low-pass Gaussian filters, and inverse of approximate local Laplacian operator are examples of such local space smoothing filters. The size of each of these region-based subdictionaries is $N^2\times N^2$, and any combination of them can be used when it is necessary.

SC Dictionary: This dictionary is also composed of two subdictionaries. For the pointlike scatterers, it contains a dictionary of shifted unit samples at every possible location in a fixed grid in the scene of interest. Curvelet is a powerful dictionary for the SR of smooth regions. However, its nonorthogonality and the large number of output coefficients make it very inefficient for implementation of our algorithm. Contourlet is an orthogonal-type curvelet without the large number of output coefficients problem. We can efficiently implement our algorithm using this dictionary. Therefore, spike-contourlet (SC) is a proper combined dictionary for joint enhancement of pointlike targets and smooth regions.

Point- and region-based (PR) and SC dictionaries are just samples of appropriate combined dictionaries to show the abilities of the new approach, and any such combined dictionary can

be used in this framework. One can try to find other combined dictionaries for different applications.

III. Experimental Results

In this section, we demonstrate the validity of the proposed method on both synthetic and real SAR scenes containing multiple types of features. We compare our results with conventional polar format imaging [1], point-enhanced nonquadratic regularization, and point-region-enhanced nonquadratic regularization [5] to show the improvements achieved. The point-region-enhanced nonquadratic regularization method incorporates both of the regularization terms introduced in [5] for pointlike targets and smooth regions simultaneously. To compare the reconstructed images quantitatively, we use the following quality metrics for real SAR scenes where we do not have the true ground image.

a) *Target-to-clutter ratio (TCR)*: as a measure of enhancement of pointlike targets with respect to the background [9]

$$\mathrm{TCR} = 20\log_{10}\left(\frac{\max_{i\in\mathcal{T}}\left(\left|(\hat{\mathbf{f}})_i\right|\right)}{\frac{1}{N_c}\sum_{j\in c}\left|(\hat{\mathbf{f}})_j\right|}\right) \tag{18}$$

where $\mathcal{T}$ is the target region, c is the clutter region, and N_c denotes the number of pixels in the clutter region.

b) *Mainlobe width (MLW)*: as defined in [9], which is a measure of the effective resolution and can be considered as a quality metric for pointlike target enhancement. In our experiments, we measure and compare the MLW of the strong point scatterers in the scene.

c) *Entropy of the full image (ENT)* [10]: entropy can be used to measure the smoothness of the probability density function of image intensities. The smoother the distribution is, the larger the entropy is [10]. Therefore, an image with smooth regions (sharp distribution) has low entropy. Therefore, entropy can be considered as a quality metric for images with enhanced smooth regions.

d) *Average speckle amplitude (ASA)* [9]: speckle complicates description of smooth regions in conventional SAR images. A measure for speckle is the standard deviation of a clutter region in the decibel-valued SAR image [9].

e) *Mean target edge strength (MTES)*: as defined in [11]: "The Sobel operator is used to generate the edge map. Then the average of all edge magnitudes above a minimum threshold is denoted as the mean target edge strength measure." Images with enhanced smooth regions should have higher values of MTES.

For synthetic scenes where the ground truth is known, we use the signal-to-noise ratio (SNR) and target localization metrics (TLM) as defined in [6].

A. Synthetic Scene Experiment

To demonstrate the capabilities of this new method and contrast it with existing methods, we consider a synthetic scene composed of both point targets and distributed targets, as shown in Fig. 1(a). The point targets have relatively smaller magnitudes than the distributed objects, and neither conventional imaging nor point-region-enhanced nonquadratic regularization could clearly distinguish them from the background. The reconstructed images in Fig. 1(e) and (f) show the success of the proposed approach in simultaneous enhancement of the two existing features in the scene. We also show the reconstructed image with a point-enhanced nonquadratic regularization method in Fig. 1(c). This method, which has a very good performance for scenes containing only pointlike features, produces a rather poor result for this experiment involving a scene with multiple types of features. The quality metrics depicted in Table I show the achieved improvement quantitatively.

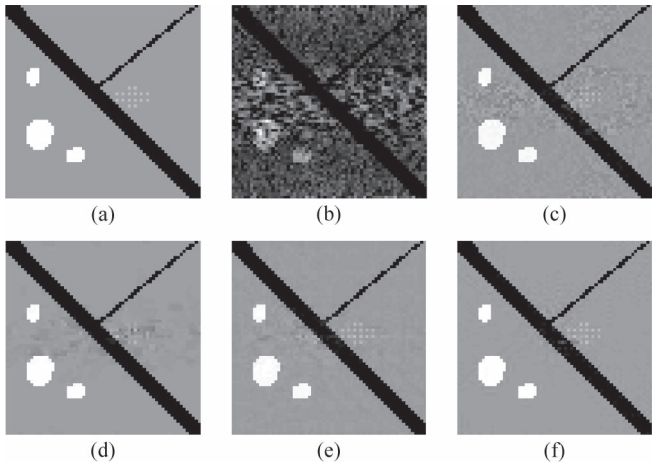

Fig. 1. Synthetic scene reconstructions: (a) synthetic scene, (b) conventional reconstruction, (c) point-enhanced nonquadratic regularization, (d) point-region-enhanced nonquadratic regularization, (e) proposed approach with PR dictionary, and (f) proposed approach with SC dictionary.

TABLE I
Computed Quality Metrics for Reconstructed Images Shown in Fig. 1

	Conventional	P-enhanced Nonquadratic	P-R-enhanced Nonquadratic	Proposed Method (PR)	Proposed Method (SC)
SNR (dB)	14.44	27.60	28.52	30.15	31.53
TLM (%)	90.40	99.29	99.38	99.43	99.53

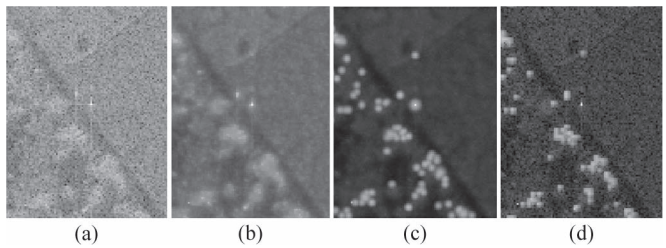

Fig. 2. Results with the ADTS data: (a) conventional reconstruction, (b) point-region-enhanced (nonquadratic regularization) reconstruction, (c) reconstruction of the proposed approach with PR dictionary, and (d) reconstruction of the proposed approach with SC dictionary.

B. Experiment With ADTS Data

In this experiment, we use a scene from the MIT Lincoln Laboratory Advanced Detection Technology Sensor (ADTS) data set [12]. It is a natural scene of size 128×128 containing trees and a corner reflector. Fig. 2(a) shows the conventional reconstruction of these data, which involves a rather poor display of the objects and regions in the scene, mostly due to severe speckle noise. The nonquadratic reconstruction of the scene is

TABLE II
COMPUTED QUALITY METRICS FOR RECONSTRUCTED IMAGES SHOWN IN FIG. 2

	Conventional	Nonquadratic	Proposed Method (PR)	Proposed Method (SC)
TCR, dB	36.23	53.50	58.77	69.18
MLW, m	0.256	0.226	0.226	0.224
ENT	3.418	0.721	0.516	0.406
ASA, dB	3.636	0.588	0.243	0.297
MTES	0.010	0.015	0.027	0.020

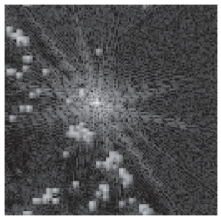

Fig. 3. Reconstruction of the ADTS data using the contourlet dictionary.

shown in Fig. 2(b), in which there is a tradeoff between enhancement of the two features of interest, namely, the spatially localized point reflectors and the spatially distributed trees and regions. Fig. 2(c) and (d) shows the reconstructed images based on the presented approach with PR and SC dictionaries, respectively. While the PR dictionary leads to improved contrast between object, background, and shadow regions compared with the conventional reconstruction, the mainlobe behavior around some objects, particularly around the corner reflector in the middle of the scene, is not satisfactory. This could be due to the use of fixed spatial smoothing filters in the region dictionary and motivates a dictionary that has a multiresolution flavor, as in the SC dictionary we use, which we present next. Fig. 2(d) shows our result with the SC dictionary, in which both the corner reflector and the smooth distributed targets (trees) are very well enhanced simultaneously. Computed quality metrics depicted in Table II show the superiority of the proposed method over the nonquadratic regularization method in terms of all quality metrics.

In order to see the effect of dictionary selection and the need for the combined dictionary presented in this letter, Fig. 3 shows the reconstructed image using the contourlet dictionary. This dictionary can sparsely represent smooth regions and cannot do the same for pointlike targets. Hence, the use of such a dictionary for scenes containing man-made targets may result in unacceptable reconstructions.

IV. DISCUSSION AND CONCLUSION

In this letter, we have considered the multiple feature-enhanced SAR image reconstruction problem. The work in [6] has developed a sparse signal representation framework for SAR imaging; however, it has used single standard signal dictionaries in the representation. In this letter, we make the point that there could be certain benefits of combining multiple potentially heterogeneous dictionaries for SAR imaging, and we demonstrate how the framework in [6] could be used in such scenarios. As an example of this line of thought, we have shown the limitations of standard dictionaries such as contourlets for enhancement of radar images containing both smooth natural regions and man-made targets, and we have proposed and shown the effectiveness of the SC dictionary as a sample combined dictionary for this purpose.

The work in [5], which originally proposed the idea of feature-enhanced sparsity-driven SAR imaging based on nonquadratic regularization, contained some hints of a similar idea of heterogeneous constraints. In particular, the approach in [5] combined so-called point enhancement and region enhancement terms in a regularized cost function. While this is similar in spirit to our idea of allowing heterogeneous features in the scene, the framework in [5] does not explicitly contain signal dictionaries, and the heterogeneous constraints are jointly applied at every spatial location in the scene, imposing what essentially are conflicting constraints at these locations. The approach we have developed in this letter resolves this issue through the use of explicit dictionaries, not requiring all of the features in the representation to be active at all spatial locations. Therefore, the work we present here provides a much more consistent approach with the objectives of multiple feature enhancement.

In addition to proposing the idea of multiple dictionaries, we have not only demonstrated the use of combinations of existing standard signal dictionaries for this task but also constructed a new region-based dictionary that could be viewed as the "synthesis" (or dictionary representation) version of the region enhancement constraint in [5].

REFERENCES

[1] W. G. Carrara, R. S. Goodman, and R. M. Majewski, *Spotlight Synthetic Aperture Radar: Signal Processing Algorithms*. Boston, MA: Artech House, 1995.
[2] S. Barbarosa, "SAR super-resolution imaging by signal subspace projection technologies," *AEU Int. J. Elect. Commun.*, vol. 50, no. 2, pp. 133–138, 1996.
[3] S. R. Degraaf, "SAR imaging via modern 2D spectral estimation methods," *IEEE Trans. Image Process.*, vol. 7, no. 5, pp. 729–761, May 1998.
[4] A. E. Brito, S. H. Chan, and S. D. Cabera, "SAR image superresolution via 2-D adaptive extrapolation," *Multidimensional Syst. Signal Process.*, vol. 14, no. 1–3, pp. 83–104, Jan.–Jul. 2003.
[5] M. Çetin and W. C. Karl, "Feature-enhanced synthetic aperture radar image formation based on nonquadratic regularization," *IEEE Trans. Image Process.*, vol. 10, no. 4, pp. 623–631, Apr. 2001.
[6] S. Samadi, M. Çetin, and M. A. Masnadi-Shirazi, "Sparse representation-based SAR imaging," *IET Radar, Sonar Navig.*, vol. 5, no. 2, pp. 182–193, Feb. 2011.
[7] M. J. Gerry, L. C. Potter, I. J. Gupta, and A. van der Merwe, "A parametric model for synthetic aperture radar measurements," *IEEE Trans. Antennas Propag.*, vol. 47, no. 7, pp. 1179–1185, Jul. 1999.
[8] S. Chen, D. Donoho, and M. Saunder, "Atomic decomposition by basis pursuit," *SIAM J. Sci. Comput.*, vol. 20, no. 1, pp. 33–61, 1999.
[9] M. Çetin, W. C. Karl, and D. A. Castañon, "Feature enhancement and ATR performance using non-quadratic optimization-based SAR imaging," *IEEE Trans. Aerosp. Electron. Syst.*, vol. 39, no. 4, pp. 1375–1395, Oct. 2003.
[10] J. Wang and X. Liu, "SAR minimum-entropy autofocus using an adaptive-order polynomial model," *IEEE Geosci. Remote Sens. Lett.*, vol. 3, no. 4, pp. 512–516, Oct. 2006.
[11] Y. Chen, G. Chen, R. S. Blum, E. Blasch, and R. S. Lynch, "Image quality measures for predicting automatic target recognition performance," in *Proc. IEEE Aerosp. Conf.*, Mar. 2008, pp. 1–9.
[12] Air Force Research Laboratory, Model Based Vision Laboratory, Sensor Data Management System ADTS. [Online]. Available: http://www.mbvlab.wpafb.af.mil/public/sdms/datasets/adts/